VPI-E-73-6
February 1973

Stress Intensity Factors for Long, Deep Surface Flaws in Plates under Extensional Fields

A. E. Harms and C. W. Smith

Department of Engineering Science and Mechanics

Prepared for:

National Aeronautics and Space Administration
Contract No. NGR 47-004-076
with NASA-Langley Research Center, Hampton, Virginia

Approved for Public Release; distribution unlimited

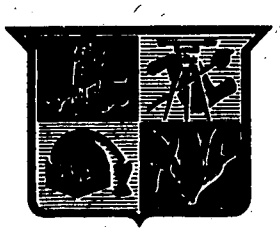

College of Engineering

Virginia Polytechnic Institute and State University

Stress Intensity Factors for Long, Deep Surface Flaws in Plates Under Extensional Fields

A. E. Harms*

and

C. W. Smith **

Department of Engineering Science and Mechanics
College of Engineering
Virginia Polytechnic Institute and State University
Blacksburg, Virginia 24061

* Graduate Research Assistant,
Department of Engineering Science and Mechanics,
Virginia Polytechnic Institute and State University
Blacksburg, Virginia 24061

** Professor of Engineering Science and Mechanics,
Virginia Polytechnic Institute and State University
Blacksburg, Virginia 24061

ABSTRACT

Using a singular solution for a part circular crack by F. W. Smith, a Taylor Series Correction Method (TSCM) was verified for extracting stress intensity factors from photoelastic data. Photoelastic experiments were then conducted on plates with part circular and flat bottomed cracks for flaw depth to thickness ratios of 0.25, 0.50 and 0.75 and for equivalent flaw depth to equivalent ellipse length values ranging from 0.066 to 0.319. Experimental results agreed well with the Smith theory but indicated that the use of the "equivalent" semi-elliptical flaw for correlating the part circular flaw results with semi-elliptical flaw results was not valid for $a/2c \ll 0.20$. Best overall agreement for the moderate ($a/t \simeq 0.5$) to deep flaws ($a/t \simeq 0.75$) and $a/2c > 0.15$ was found with a semi-empirical theory due to J. C. Newman when compared on the basis of equivalent flaw depth and area. The Smith theory, when correlated on the basis of flaw depth and area, appears to yield reasonable estimates (within 10%) of the SIF for flat bottomed flaws for the geometries studied here.

CONTENTS

FIGURES

TABLE

NOMENCLATURE

$\sigma_{nn}, \sigma_{zz}, \tau_{nz}$	- Stress components in a plane normal to the crack border (psi)
K_I	- Mode I Stress Intensity Factor (lbs./[in]$^{3/2}$)
r, θ	- Polar coordinates (inches, radians)
a	- Flaw depth (inches)
A	- Radius of penetrating circle (inches)
2c, 2m	- Flaw length in plate surface (inches)
t	- Plate thickness (inches)
ϕ	- Eccentric angle of ellipse (radians)
σ_0'	- Normal stress parallel to crack surface in singular region (psi)
n'	- Fringe order
f	- Material fringe value (lbs/in/order)
τ_{max}, τ_m	- Maximum shearing stress in plane perpendicular to crack border (psi)
τ_{mo}	- Maximum remote shearing stress in plane perpendicular to crack border at plate surface (psi)
K_{ap}	- Apparent stress intensity factor (lbs/[in]$^{3/2}$)
K_{Sm}	- Theoretical stress intensity factor (lbs/[in]$^{3/2}$)
K_{TSCM}	- Approximate stress intensity factor (lbs/[in]$^{3/2}$)

INTRODUCTION

The first analytical expression for stress intensity factors due to surface flaws was apparently developed by G. R. Irwin [1] for a semi-elliptical flaw in a half space in 1962. His result was obtained by utilizing the crack opening displacements obtained by Green and Sneddon [2] for an embedded elliptical flaw. Irwin's result contained empirical corrections for free surface and plasticity effects. It did not contain back surface effects, which have since been found to be quite important, especially for deep flaws. A number of expressions were subsequently developed for accounting for the back surface effect. One of the better approximate theories which illustrates a typical approach involving independent front and back surface corrections is due to F. W. Smith [3]. He assumed that the stress intensity factors for the semi-elliptical and semi-circular cracks were related in the same way as the embedded elliptical and penny-shaped cracks, and empirically adjusted the relations so the solution would coalesce with semi-circular and edge crack solutions. Following this work, Smith and Alavi [4], using a Schwartz Alternating Technique developed by Smith, Emery and Kobayashi [5], obtained the stress intensity factor (SIF) at the point of maximum flaw penetration for a part circular crack in a half-space. This study was extended by Smith and Thresher [6] in 1969 to the finite thickness plate. More recently, Smith [7] has correlated the part circular flaw analysis with experimental results for semi-elliptical surface flaws. During the same period, Kobayashi and his associates have been studying the semi-elliptical surface flaw problem quite extensively [8],[9],[10] and Rice and Levy [11], by replacing the flaw with a continuous non-linear spring and utilizing an edge crack solution, have developed an

approximate solution to the problem. Very recently, Shah and Kobayashi [12] have presented a survey of available approximate solutions to the problem.

The surface flaw problem is a three-dimensional problem which has remained intractable to a complete solution for some years. Approximate theories such as some of those mentioned above are available which provide approximate theoretical stress intensity factors over a complete range of semi-elliptical flaw and plate depth geometries. However, experimental verification of such theories has not been obtained for certain geometrical ranges, especially the range of fairly long and deep flaws. A fairly comprehensive collection of both analytical and experimental results are found in Ref. [12] and utilization of these works to develop fracture criteria is due to Newman [13]. It is the purpose of the present study to develop a reliable photoelastic procedure for determining the stress intensity factor experimentally and to use this procedure to study stress fields for long, deep cracks and obtain the corresponding stress intensity factors.

ANALYTICAL CONSIDERATIONS

The theory of fracture mechanics predicts that there is a zone near the tip of a crack border where the stress field in a plane perpendicular to the crack border can be represented by means of a field theory consisting of two degrees of freedom, or two parameters. These parameters are the stress intensity factor (SIF) represented by K_I, and the normal stress in the direction of crack extension σ_0'. K_I is the parameter of the singular stress field and σ_0' is a parameter of the regular part of the stress field and is considered to be a constant near the crack tip. A considerable amount of work [14] - [22] has been done in recent years in which the photo-

elastic method has been used to study crack tip stress fields and to obtain stress intensity factors from photoelastic data [23] - [30]. In photoelasticity, one obtains measurements in the form of stress fringes which are proportional to the maximum in-plane shear stress. When one computes theoretical fringes from the two-degree of freedom system of equations mentioned above, one obtains eccentric fringe loops which intersect at the tip of the branch cut representing the crack tip. These loops are controlled by K_I but are subject to distortion due to σ_0' [28]. The fringe loops, however, always tend to separate furthest along or near a line normal to the crack surface and passing through the crack tip. For this reason, the authors have elected to measure fringe loop heights along such lines, since clearest fringe order discrimination is always best in this neighborhood near the crack tip. Thus, all stresses obtained from the stress field equations will be evaluated along $\theta = \pi/2$, representing the above mentioned direction.

Beginning with the stress components in a plane normal to the crack border in the Mode I form for the two-degree of freedom system:

$$\sigma_{nn} = \frac{K_I}{(2\pi r)^{1/2}} \cos\frac{\theta}{2}\left(1 - \sin\frac{\theta}{2}\sin\frac{3\theta}{2}\right) - \sigma_0'$$

$$\sigma_{zz} = \frac{K_I}{(2\pi r)^{1/2}} \cos\frac{\theta}{2}\left(1 + \sin\frac{\theta}{2}\sin\frac{3\theta}{2}\right) \qquad (1)$$

$$\tau_{nz} = \frac{K_I}{(2\pi r)^{1/2}}\left(\sin\frac{\theta}{2}\cos\frac{\theta}{2}\cos\frac{3\theta}{2}\right)$$

where the notation is given in Figure 1.

We may substitute Eqs. (1) into

$$\tau_{max}^2 = \frac{1}{4}\left\{(\sigma_{nn} - \sigma_{zz})^2 + 4\tau_{nz}^2\right\} \tag{2}$$

and evaluate τ_{max}^2 along $\theta = \pi/2$ to yield

$$\tau_{max}^2 = \frac{K_I^2}{8\pi r} + \frac{K_I\sigma_0'}{4(\pi r)^{1/2}} + \frac{\sigma_0'^2}{4} \tag{3}$$

which may be combined with the stress-optic law:

$$\tau_{max} = \frac{n'f}{2t} \tag{4}$$

in order to obtain an equation involving the unknowns n', r, K_I and σ_0'. By measuring pairs of values of n',r for two different fringes, two equations result from which σ_0' can be eliminated to solve for K_I. By using all pairs of fringe loops, a set of values of K_I result which may be data conditioned to yield accurate results. The details of the method are described in References [28] and [29] and the method has also been employed by Kobayashi and his associates [31], [32].

The two-degree of freedom method is quite adequate for analyzing photoelastic data when the data are taken in the zone dominated by the crack surface boundaries only. However, when other boundaries are near, as is the case with deep flaws, or if other boundaries or loadings exert strong effects on the crack tip region, the field dominated by the two parameter stress system may be severely constricted [33] and the range of photoelastic data may lie outside of this range. In such cases, additional degrees of freedom must be provided in the analytical expressions for the stresses in order to account for such effects. A simple way of achieving this result is to apply a Taylor Series Correction to τ_{max} in the form

$$\tau_{max} = \frac{A}{r^{1/2}} + B + \sum_{n=1}^{m} C_n r^n \qquad (5)$$

which may be compared to the two degree of freedom approach by rewriting Equation (3) as:

$$\tau_{max} = \frac{A'}{r^{1/2}} + B' + C' r^{1/2} \text{ where } B' = f(A', C') \qquad (6)$$

The Taylor series is expressed in terms of r^n rather than $r^{n/2}$ to enhance convergence.

For problems in which all data are taken in the valid singular zone, Equation (6) would be appropriate. The corresponding form for Equation (5) would consist of only the first two terms and the difference in the two equations may be regarded as a truncation error. The Taylor Series Correction Method (TSCM) when applied to two dimensional problems, is equivalent to expanding the stress components in terms of a Williams stress function [34] and computing τ_{max} from Equation (2).

The computer program utilized by the TSCM adds terms in the Taylor Series one at a time, and recomputes A, B, C_n by a least squares procedure after each new term is added. Convergence of A to its proper value is rapid and in the present study always occurred in less than six terms. However, the program must be accompanied by a truncation criterion, for if it is allowed to continue, random experimental error will eventually lead to unreliable values of A. The authors have found that by truncating the series when the m^{th} term changes the value of τ_{max} by an amount comparable to the estimated experimental error, good results are usually obtained. If the experimental error lies between two terms, say $m^{th} - 1$ and m^{th}, corresponding K_I values may be averaged. It is expected that, as experience is gained with the method, a more precise truncation criterion can be

developed. Verification of the convergence of the method is described in Reference [30].

THE EXPERIMENTS

A set of photoelastic experiments employing the stress freezing technique was designed to obtain photoelastic data on the stress fields near points of deepest flaw penetration in cracked specimen models of various crack and plate depth geometries. Pilot tests revealed that it would not be feasible to use "natural" cracks due to the fact that the low value of the threshold K_{IC} for stress freezing photoelastic materials tends to produce premature failures in the stress freezing process for deep flaws under tensile loads. Since F. W. Smith has correlated his part circular crack theory with experimental data on semi-elliptical flaws by matching the flaw depth and curvatures, it was decided to produce part circular cracks with a 0.006" thick circular saw, and compare the result with the Smith theory directly to validate the experimental result, and then to convert the experimental data to semi-elliptical form on the basis of matching depth and curvature, depth and length, or depth and area for comparison with other theories. These theories are briefly described in Appendix A.

Materials and Models - Two stress freezing materials were used in the experiments. They were Hysol 4290 and PLM-4B, the former manufactured by Hysol Corporation of Olean, New York, and the latter by Photoelastic Inc. of Malvern, Pa. Both materials possess a low material fringe value in the rubbery range and were relatively easy to machine. The thermal cycles for annealing and stress freezing were:

Hysol: Heat to 280°F in 2 hours; soak for 6 hours. Cool at 5°F/hr. to room temperature (2-day cycle).

PLM-4B: Heat to 260°F in 4 hours; soak for 16 hours. Cool at 3°F/hr. to room temperature (4-day cycle).

The procedure used for the Hysol was to rough cut, anneal, saw in the crack and then stress freeze. For the PLM-4B, surfaces were milled first, then the crack was sawed in, followed by stress freezing. Holes were drilled before stress freezing near the ends of each plate to receive pins through which the loads were applied. A typical specimen is shown in Figure 2.

Loading System and Procedure - Test specimens were suspended and loaded through nylon lines passing through fishing swivels to pins in small holes near the plate ends. The lines were "tuned" under full load to insure proper load distribution. The load was then removed and the stress freezing cycle was begun. The live load was applied near the end of the thermal soak, and the specimens were cooled, freezing in the stresses and deformations. A photo of the test set-up is shown in Figure 3 and a flaw is shown after stress freezing in Figure 4. Slicing was then done according to Figure 5 and the slices were placed in an oil bath of the same index of refraction as the model material, between two partial mirrors of a fringe multiplication system in a circular polariscope. Stress fringes were photographed. Figure 6(a) shows a typical unmultiplied fringe pattern and Figure 6(b) shows the fifth multiple. The unmultiplied pattern was used to locate integral or half-integer order fringes. In Figure 6, fringe patterns are in a bright field.

RESULTS AND DISCUSSION

Data on all tests are found in the upper part of Table I. The part circular flaw tests were grouped according to a/t values as follows:

Group I	$a/t \simeq 0.25$	Tests 1, 2 and 3
Group II	$a/t \simeq 0.50$	Tests 4, 5, 6 and 7
Group III	$a/t \simeq 0.75$	Tests 8, 9, 10 and 11.

Finally, deep, long, flat bottom cracks with part circular edges were tested in Group IV, Tests 12 and 13. Experimental values of maximum in-plane shearing stresses were determined directly from the fringe patterns along lines normal to the crack surface and passing through the crack tip. These values were used in the TSCM in order to determine the coefficients in Equation (6) and the experimental SIF. The raw data are shown in Figures 7 and 8 for each test group together with the fitted curves from the TSCM. In Figures 9 through 12 the data are replotted to show convergence trends. It might be remarked that, if the data formed a horizontal straight line in these latter figures, a one term expansion of Equation 5 would be sufficient. For a straight inclined line, a two term expansion would be adequate. In either of these cases, one would be well within the zone dominated by the singular stresses.

The extent to which the experimentally determined K_{TSCM} differs from that predicted by the Smith part circular crack theory is measured from the ordinate intercept. A value of unity would correspond to exact agreement between theory and the experimental result. The fitted curve used for extrapolation to the origin comes from the TSCM.

As can be seen from Figure 9, non-linearity is not strong, but is present to some degree in the shallow flaws. (Group I) For the moderately deep flaws of Group II, non-linear effects are stronger, and larger errors

in K_I would be obtained if linear data extrapolations were used (Fig. 10). For deep part circular flaws shown in Figure 11, a proper method of extrapolation is even more important. The indications are, that as the flaw grows deeper and longer, the zone dominated by the singular term shrinks in size and, moreover, it is more difficult to measure valid data close to the crack tip. However, by accepting the data where they can be obtained most accurately, valid trends can be obtained.

In order to cover the range of geometry studied in this program, it was necessary to extrapolate from the curves generated by the Smith theory. All extrapolation was linear.

The poorest agreement between the experimental results and the Smith theory for part circular flaws was about 10%. (Table I) However, the value of Poisson's ratio for the test materials was 0.49 as compared to a value of 0.25 used in the Smith theory. Estimates by F. W. Smith and independently by the authors indicate that this order of difference might be expected to increase K_I by 5 to 10%, depending upon the geometry. On this basis, the experimental error is judged to be within ±5%.

For purposes of comparison with theories for semi-elliptical flaws, results for the part circular flaws were converted to equivalent semi-elliptical flaws by equating maximum flaw depths and i) curvatures at maximum flaw depth, ii) flaw areas, and iii) flaw surface lengths. These comparisons are shown in Table I. The general trend is to increase the respective theoretical K's as one computes equivalent flaws, proceeding i) through iii). Differences between theoretical predictions for the same flaw geometry were usually within 10% but, in some cases, exceeded 20% (e.g. Shah-Kobayashi vs Rice-Levy for equal flaw depth and length Test 1).

Similarly, differences between results predicted by the same theory for cases i, ii) and iii) were generally smaller than 10%, but for some cases in Group III, were quite large, [e.g., Test 8 Rice-Levy i) vs. Rice-Levy iii)]. Moreover, substantial differences are observed between the theory of F. W. Smith and the other theories for equivalent geometries (e.g., Tests 7, 10 and 11) for the longer or deeper, and longer and deeper flaws, as well as for Group I.

In correlating his theory with experimental results, Smith compared it with "equivalent" semi-elliptical surface flaws at equal flaw depth and curvature. He found that the fracture toughness data scatter about the "equivalent" theoretical curve was $\pm$ 10% for a/2c values of 0.21 to 0.42 and over a full range of a/t from nearly zero to unity. Thus, Group I and Tests 7, 11, 12 and 13 fall outside the range of Smith's correlation. However, Tests 7 and 11 were judged close enough to Smith's range of a/2c values to be included. The results as displayed in Table I show that the tests in Group I do not, in fact, agree with any of the approximate theories based on any of the three methods of converting part-circular results to semi-elliptical results. This suggests that "equivalent" comparisons between part-circular and semi-elliptical flaw results are not valid in the Group I range. Agreement between experiment and "equivalent" elliptical flaw results was fair for Group II and was best, in general, with the Newman Theory, using either equivalent lengths or areas and flaw depths. The agreement between the Newman Theory and experimental results in Group III was excellent, using equivalent flaw depth and area.

The results of Group IV are of interest due to the lack of adequate experimental data for long deep surface flaws. These geometries consisted of flat bottomed cracks with part-circular sides. Since these geometries

were not semi-elliptical and were not within the range of equivalent cracks correlated by F. W. Smith, it was decided to compare the experimental results with the Smith theory directly as well as with equivalent semi-elliptical flaws of the same flaw depth and area and length, respectively. Figure 12 results are normalized with respect to the Smith theory, based upon equal depth and area, even though this theory does not necessarily apply to the flat bottomed crack geometry. Nevertheless, extrapolation trends would not be expected to diverge significantly from those for the long, deep part circular cracks. Thus, the extrapolation of Figure 12 is judged to be correct, and suggests that if reasonably valid data are taken, even substantially outside the singular zone, the TSCM will predict proper extrapolation trends. It is always desirable, however, to verify extrapolation trends on existing K solutions as is done here with Smith's theory.

These results seem to indicate that the Smith theory, based on equivalent depth and area, will give good estimates (within 10%[a]) of the experimental SIF. It may be conjectured that the flat bottom crack may be used to experimentally study long crack geometries and that the Smith theory based upon equivalent depth and area may be used to estimate SIF values here. However, further experiments are needed to confirm this conjecture.

---

[a]Although Test 13 (Fig. 12) shows a 12% difference, about half of this is believed due to differences in Poisson's Ratio noted earlier for which no adjustments in data were made.

SUMMARY AND CONCLUSIONS

A series of three dimensional stress freezing photoelastic experiments were conducted on plates containing part circular surface flaws and a Taylor Series Correction Method (TSCM) was used to predict values of the SIF. Results were compared with a theory due to F. W. Smith for verification and, using several methods, to "equivalent" semi-elliptical flaw theories of Kobayashi and Shah, Rice and Levy and Newman. Tests were also run on two geometries involving flat bottom cracks with part circular ends for which similar "equivalent" comparisons were made with the Smith theory. The above comparisons led to the following conclusions:

a) The Taylor Series Correction Method (TSCM) will yield good estimates of the SIF when applied to stress frozen models of part circular cracks.

b) Prediction of SIF values for semi-elliptical cracks for fairly long, shallow flaws $a/t \simeq 0.25$ (Group I) by the "equivalent" flaw method from part circular flaw theory leads to substantial discrepancies from results of other semi-elliptical flaw theories.

c) For moderate ($a/t \simeq 0.5$) to deep ($a/t \simeq 0.75$) flaws of moderate to fairly substantial length (Groups II and III), the Newman theory for semi-elliptical flaws of the same depth and area yields SIF predictions to within 10% (in most cases) of experimental results.

d) For long, deep, flat bottomed cracks, the Smith theory for a part circular flaw of equal area and depth gave a reasonable estimate (within 10%) of the SIF for the geometries studied here.

On the basis of the limited information presented here, it may be conjectured that the rather large difference between semi-elliptical flaw results for very low values of a/2c (say 0.05 or less) and the edge crack

($a/2c \to 0$) as discussed by Underwood [35] may in fact exist and could be verified to a limited extent experimentally using flat bottomed cracks with long flat zones. However, further experiments would be necessary to support this conjecture.

The results cited here should be regarded as approximations to a complex three dimensional problem. There are many potential sources of error, but these have been assessed and the included results are believed to appropriately reflect the three dimensional effects inherent in the problems studied. Extrapolation to problems of significantly different geometry is not recommended.

ACKNOWLEDGEMENT

The authors are indebted to F. W. Smith, R. C. Shah, A. S. Kobayashi, J. R. Rice, N. Levy and J. C. Newman for their contributions to the literature which were used as a basis for this work. The assistance of M. A. Schroedl and J. J. McGowan with computer programming is also appreciated. Finally, the suggestions of J. C. Newman and C. C. Poe and the encouragement and support of D. Frederick are gratefully acknowledged. This research was supported by NASA under NGR-47-004-07C with NASA Langley, Hampton, Virginia.

REFERENCES

1. Irwin, G. R., "Crack Extension Force for a Part Through Crack in a Plate," Journal of Applied Mechanics, Vol. 29, No. 4, Trans. ASME, Vol. 84, Series E, Dec. 1962, pp. 651-654.

2. Green, A. E. and Sneddon, I. N., "The Distribution of Stress in the Neighborhood of a Flat Elliptical Crack in an Elastic Solid," Proceedings of the Cambridge Philosophical Society, Vol. 46, 1950, pp. 159-163.

3. Smith, F. W., "Stress Intensity Factors for a Semi-Elliptical Surface Flaw," Structural Development Research Memorandum No. 17, The Boeing Co., Seattle, Washington, Aug. 1966.

4. Smith, F. W. and Alavi, M. J., "Stress Intensity Factors for a Part Circular Surface Flaw," Proc. of First International Conference on Pressure Vessel Technology, Delft, The Netherlands, 1969.

5. Smith, F. W., Emery, A. F., and Kobayashi, A. S., "Stress Intensity Factors for Semi-Circular Cracks - Part 2 Semi-Infinite Solid," Journal of Applied Mechanics, Vol. 34, Dec. 1967, Trans. ASME, Vol. 89, Series E, 1967, pp. 953-959.

6. Thresher, R. W. and Smith, F. W., "Stress Intensity Factors for a Surface Crack in a Finite Solid," ASME Paper No. 71-APMW-6 (in press) J. of Applied Mechanics.

7. Smith, F. W., "Stress Intensity Factors for a Surface Flawed Fracture Specimen," TR-1, Dept. of Mechanical Engineering, Colorado State Univ., September 1971.

8. Kobayashi, A. S. and Moss, W. L. "Stress Intensity Magnification Factors for Surface Flawed Tension Plate and Notched Round Tension Bars," Proceedings of the Second International Conference on Fracture, Brighton, England, 1969.

9. Shah, R. C. and Kobayashi, A. S., "Stress Intensity Factor for an Elliptical Crack Under Arbitrary Normal Loading," Journal of Engineering Fracture Mechanics 3, 1, July 1971, pp. 71-96.

10. Shah, R. C. and Kobayashi, A. S., "Stress Intensity Factors for an Elliptical Crack Approaching the Surface of a Semi-Infinite Solid," (in press) International Journal of Fracture Mechanics.

11. Rice, J. R. and Levy, N., "The Part Through Surface Crack in an Elastic Plate, ASME Paper No. 71-APM-20 (in press) J. of Applied Mechanics.

12. Shah, R. C. and Kobayashi, A. S., "On the Surface Flaw Problem," (in press) Proceedings of ComCAM Symposium on the Surface Flaw Applied Mechanics Division of ASME Winter, 1972.

13. Newman, J. C., "Fracture Analysis of Surface and Through Cracked Sheets and Plates," (in press) J. of Engineering Fracture Mechanics, 1973.

14. Post, D., "Photoelastic Stress Analysis for an Edge Crack in a Tensile Field," Proceedings, Society for Experimental Stress Analysis 12, 1, pp. 99-116 (1954).

15. Wells, A. A. and Post, D., "The Dynamic Stress Distribution Surrounding a Running Crack - A Photoelastic Analysis," Proceedings, Society for Experimental Stress Analysis 16, 1, pp. 69-92 (1958).

16. Irwin, G. R., Discussion of Reference [15], Proceedings, Society for Experimental Stress Analysis 16, 1, pp. 69-92 (1958).

17. Fessler, H. and Mansell, D. O., "Photoelastic Study of Stresses Near Cracks in Thick Plates," Journal of Mechanical Engineering Science 4, 3, pp. 213-225 (1962).

18. Kerley, B., "Photoelastic Investigation of Crack Tip Stress Distributions" GT-5 Test Report Document No. 685D 597, The General Electric Co. (March 15, 1965).

19. Dixon, J. R. and Strannigan, J. S., "A Photoelastic Investigation of the Stress Distribution in Uniaxially Loaded Thick Plates Containing Slits," NEL Report No. 288, National Engineering Laboratory, Glasgow, Scotland (May, 1967).

20. Liebowitz, H., Vanderveldt, H., and Sanford, R. J., "Stress Concentrations Due to Sharp Notches," Experimental Mechanics 7, 12, pp. 513-517 (Dec., 1967).

21. Smith, D. G. and Smith, C. W., "A Photoelastic Evaluation of the Influence of Closure and Other Effects upon the Local Bending Stresses in Cracked Plates," International Journal of Fracture Mechanics 6, 3, pp. 305-318 (September, 1970).

22. Smith, D. G. and Smith, C. W., "Influence of Precatastrophic Extension and Other Effects on Local Stresses in Cracked Plates under Bending Fields," Experimental Mechanics 11, 9, pp. 394-401 (Sept., 1971).

23. Bradley, W. B. and Kobayashi, A. S. "An Investigation of Propagating Cracks by Dynamic Photoelasticity," J. of Experimental Mechanics 10, 3, pp. 106-113 (March, 1970).

24. Bradley, W. B. and Kobayashi, A. S., "Fracture Dynamics - A Photoelastic Investigation," J. of Engineering Fracture Mechanics 3, 3, pp. 317-332 (October, 1971).

25. Marloff, R. H., Leven, M. M., Johnson, R. L., and Ringler, T. N., "Photoelastic Determination of Stress Intensity Factors," Experimental Mechanics 11, 12, pp. 529-539 (December, 1971).

26. Smith, D. G. and Smith, C. W., "Photoelastic Determination of Mixed Mode Stress Intensity Factors," VPI-E-70-16, June 1970. J. of Engineering Fracture Mechanics 4, 2, pp. 357-366 (June 1972).

27. Marrs, G. R. and Smith, C. W., "A Study of Local Stresses Near Surface Flows in Bending Fields," Stress Analysis and Growth of Cracks ASTM STP 513, pp. 22-36 (October, 1972).

28. Schroedl, M. A., McGowan, J. J. and Smith, C. W., "An Assessment of Factors Influencing Data Obtained by the Photoelastic Stress Freezing Technique for Stress Fields Near Crack Tips," VPI-E-72-6 (in press) J. of Engineering Fracture Mechanics.

29. Schroedl, M. A., and Smith, C. W., "Local Stresses Near Deep Surface Flaws Under Cylindrical Bending Fields (in press) Proc. of Sixth National Symposium on Fracture Mechanics (September 1972).

30. Schroedl, M. A., McGowan, J. J. and Smith, C. W., "Determination of Stress Intensity Factors from Photoelastic Data with Application to Surface Flaw Problems," (in press) VPI-E-73-1 Report (1973).

31. Kobayashi, A. S., Wade, B. G., Bradley, W. B. and Chiu, S. T., "Crack Branching in Homalite-100 Sheets" TR-13, Dept. of Mechanical Engineering, College of Engineering University of Washington (June 1972).

32. Kobayashi, A. S. and Wade, B. G., "Crack Propagation and Arrest in Impacted Plates," RT-14, Dept. of Mechanical Engineering, College of Engineering, University of Washington (July 1972).

33. Wilson, W. K., "Geometry and Loading Effects on Elastic Stresses at Crack Tips," Research Report G7-107-BTLPV-R1, Westinghouse Research Labs, Pittsburgh, Pa. 15235 (July 1967).

34. Williams, M. L., "On the Stress Distribution at the Base of a Stationary Crack," J. Ap. Mech. 24, pp. 109-114 (1957). See also Ref. [24].

35. Underwood, J. H., Comments on the Paper by R. C. Shah and A. S. Kobayashi, "Stress Intensity Factor for an Elliptical Crack Approaching the Surface of a Semi-Infinite Solid," J. of Elasticity 2, 2, (June 1972).

36. Miyamoto, H. and Miyoshi, T., "Analysis of Stress Intensity Factor for a Surface-Flawed Tension Plate," High Speed Computing of Elastic Structures Proc. of Symposium of IUTAM, Univ. de Liege, 1971, pp. 137, 155.

APPENDIX A - Theoretical Solutions

I - The Smith theory (for a part circular crack) Ref. [7] Using two solutions,

i) The penny shaped crack in an infinite body subjected to a crack surface pressure and

ii) A half space loaded with surface tractions on a rectangular portion of the boundary,

Smith applied the Schwartz Alternating Technique utilizing solution i) on the crack surface and solution ii) on the front face. As he iterated back and forth, he collected residuals on the back face and then iterated between the crack surface and the back face. The above procedure was repeated until residuals were negligible. Smith expressed his results in the form:

$$K_I = \frac{2}{\pi} M \sigma_0 (\pi A)^{1/2} \qquad (A\text{-}1)$$

where:

σ_0 is the remote extensional stress

A is the radius of the penetrating circle

M = M(a/t, A-a/a) for the point of maximum flaw penetration

Results of this theory are estimated by the author to be well within 5% of the correct value at the point of maximum flaw penetration. Results are available for values of Poisson's ratio of 0.25 and 0.39.

Correlation with experimental values of K_{IC} for natural semi-elliptic flaws was obtained by matching flaw depth and curvature over a range of a/2c of 0.20 to about 0.40. Data scatter of experimental data was within $\pm$ 10%.

II - The Shah-Kobayashi theory (for a semi-elliptical crack) Ref. [10], [12] Using two solutions:

i) The embedded elliptical flaw in an infinite body with a pressure on the crack surface, and

ii) A half space loaded with surface tractions on its surface,

Shah and Kobayashi applied the Schwartz Alternating Technique, utilizing these solutions and iterating between the crack surface and the back surface of the plate. However, instead of collecting residuals on the front face and including them in the iteration process as Smith did, they utilized a front surface correction factor developed by Kobayashi and Moss [8]. Thus, the influence of coupling of the front and back surface effects is not included. It might be added that such an inclusion appears more complex for the elliptical than for the part circular problem.

The authors expressed their result in the form:

$$K_I = M_K \sigma_0 \frac{\sqrt{\pi a}}{\Phi} \qquad \text{(A-2)}$$

σ_0 is the remote extensional stress

a is the flaw depth

Φ is a complete elliptic integral of the second kind, i.e.,

$$\Phi = \int_0^{\pi/2} \left\{1 - \left(\frac{c^2 - a^2}{c^2}\right) \sin^2\phi\right\}^{1/2} d\phi$$

where 2c is the major diameter of the semi-elliptic flaw. (Figure 2)

M_K = Product of back and front surface corrections.

Results were obtained using a value of Poisson's Ratio of 0.30. Correlations were made with fracture toughness data which contained a fair amount of scatter. Correlation with finite element results of Miyamato and Miyoshi [36] was excellent for a/2c = 0.10, a/t = 0.30 and reasonably

good for a/2c = 0.10, a/t = 0.8 and a/2c = 0.30 and a/t = 0.8.

III - The Rice-Levy theory (for long surface flaws) Ref. [11].

Rice and Levy replaced the plate cross section containing a surface flaw with a continuous spring,and employed two dimensional generalized plane stress and Kirchoff-Poisson plate bending theories to account for combined extension and bending. The compliance of the surface flaw was set equal to the compliance of an edge crack under plane strain with the same flaw depth. The mathematical formulation was reduced to two coupled integral equations which were solved to yield values of the thickness averaged extensional and nominal bending stresses as a function of flaw length. For the point of maximum flaw penetration, they computed the stress intensity factor as:

$$K_I = t^{1/2}[\bar{\sigma}_0 g_t + \bar{m}_0 g_b] \qquad \text{(A-3)}$$

where

$$\bar{\sigma}_0 = \frac{N_{22}(0,0)}{t} = \frac{1}{t}\int_{-\frac{t}{2}}^{+\frac{t}{2}} \sigma_{22}(0,0,x_3)dx_3$$

$$\bar{m}_0 = \frac{6M_{22}(0,0)}{t^2} = \frac{1}{t^2}\int_{-\frac{t}{2}}^{+\frac{t}{2}} x_3\sigma_{22}(0,0,x_3)dx_3$$

g_t, g_b = functions of a/t for extension and bending respectively as obtained for an edge crack.

The x_1x_2 plane is the middle plane of the plate.

The x_3 axis passes through point of maximum flaw penetration.

N_{22}, M_{22} = normal force and bending moment per unit thickness.

$\bar{\sigma}_0$, $\bar{m}_0$ = thickness average stresses for the surface flaw at the location of maximum flaw penetration.

Although presumably limited to cracks which were long relative to plate depth, their results compared favorably with the Smith-Alavi theory for a part circular surface flaw for the case of remote tension, and for a nearly semi-circular flaw geometry.

IV - Newman's theory Ref.[13]

The Neuber theory for an elastic plastic material was generalized in a quasi-empirical manner so as to apply to a crack in a finite plate subjected to tensile loading. A fracture criterion involving two material parameters is developed, utilizing the results of several earlier theories. Newman utilized Irwin's [1] expression for the stress intensity factor for part through cracks in the form of Equation A-2. His correction factor, M_e, however, was an empirical expression adjusted to account for the finite width effect as well as front and back surface corrections. His equation may be written as:

$$K_I = M_e \frac{\sigma_0}{\Phi} \sqrt{\pi a} \qquad \text{(A-4)}$$

M_e is a coefficient which includes front and back surface corrections as well as a finite width correction.

Newman shows extensive correlation for his fracture criterion for a variety of materials and crack geometries.

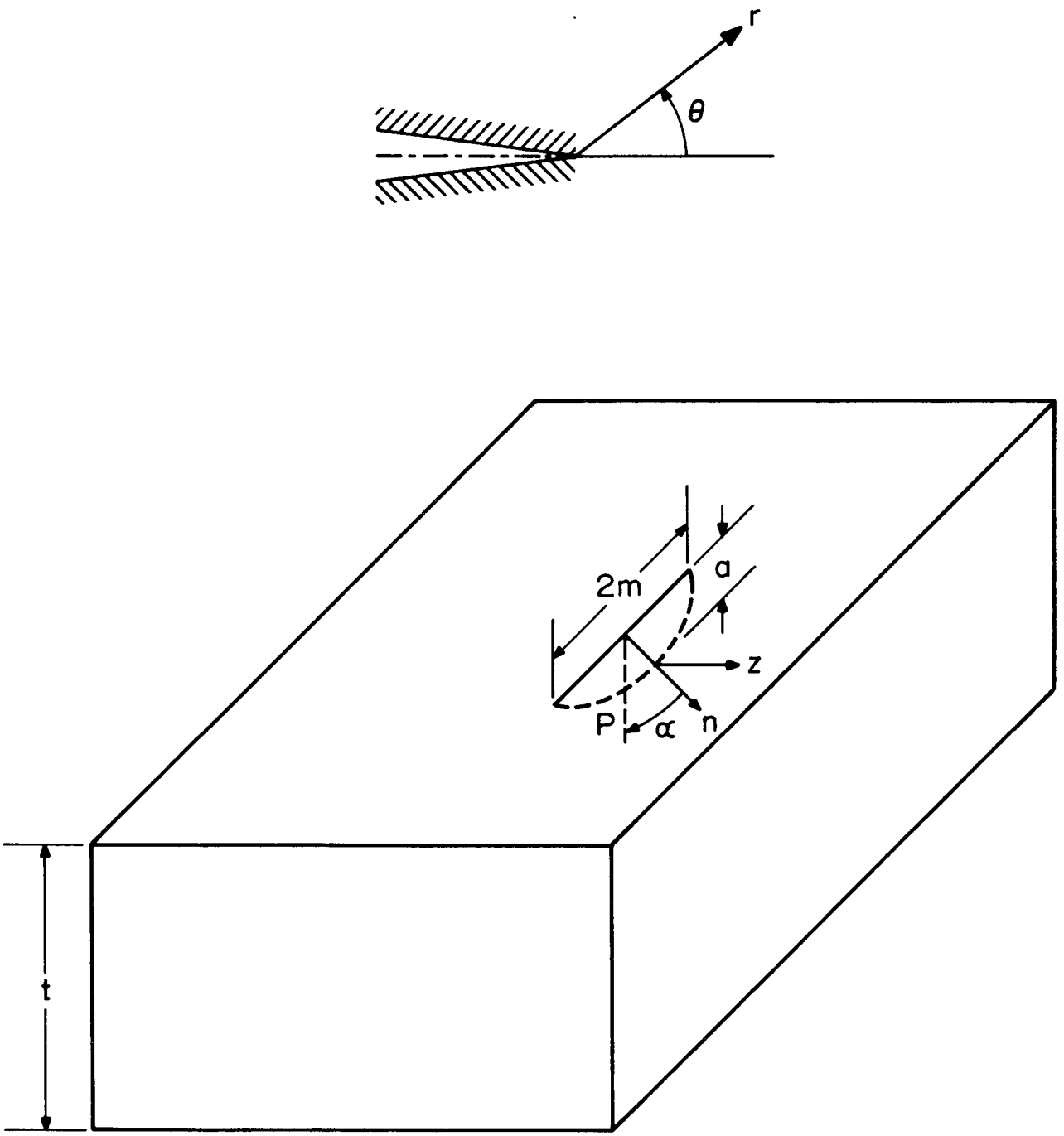

Figure 1. Notation for Stress Field Near Crack Tip

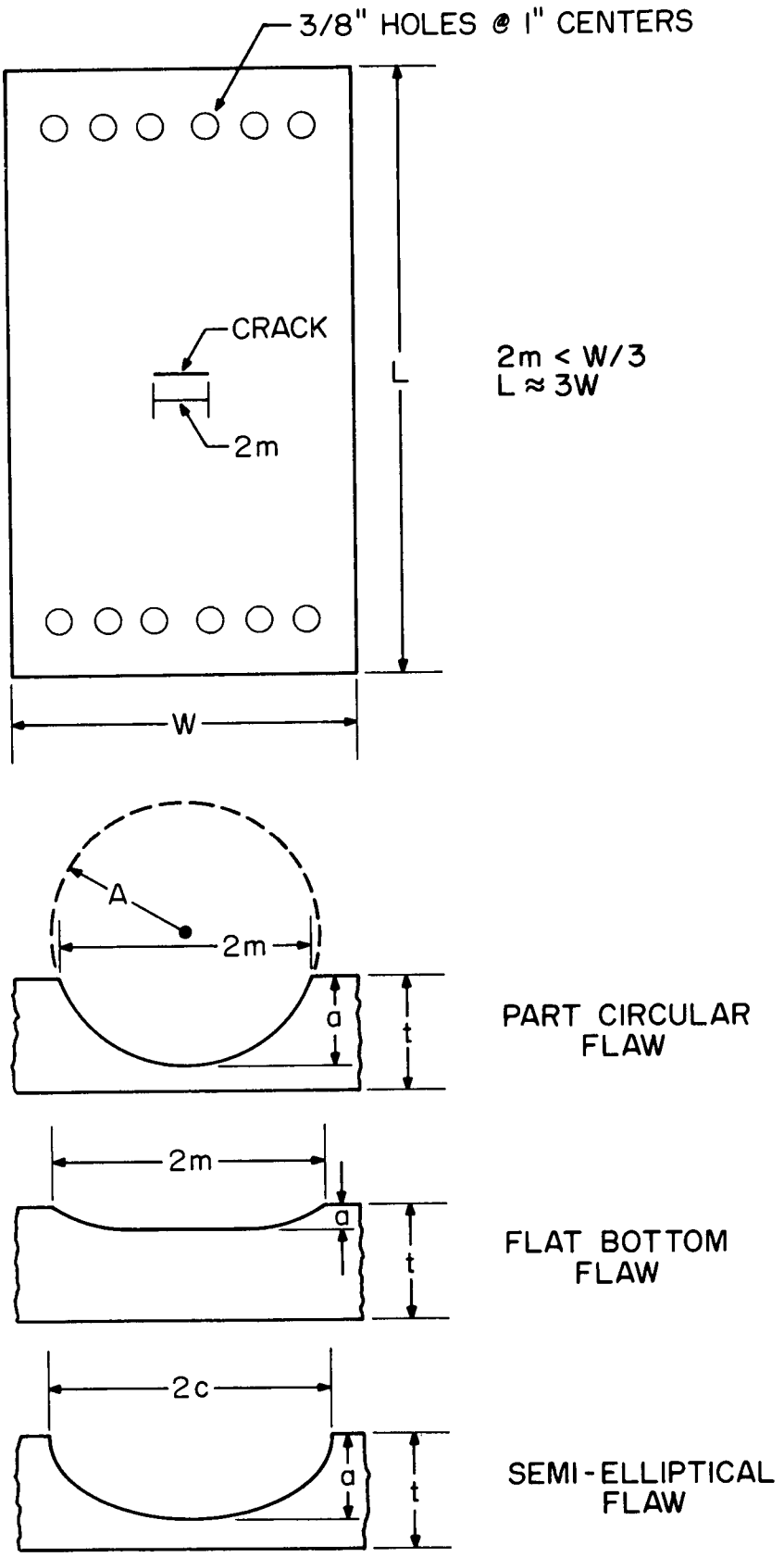

Figure 2. Typical Specimen

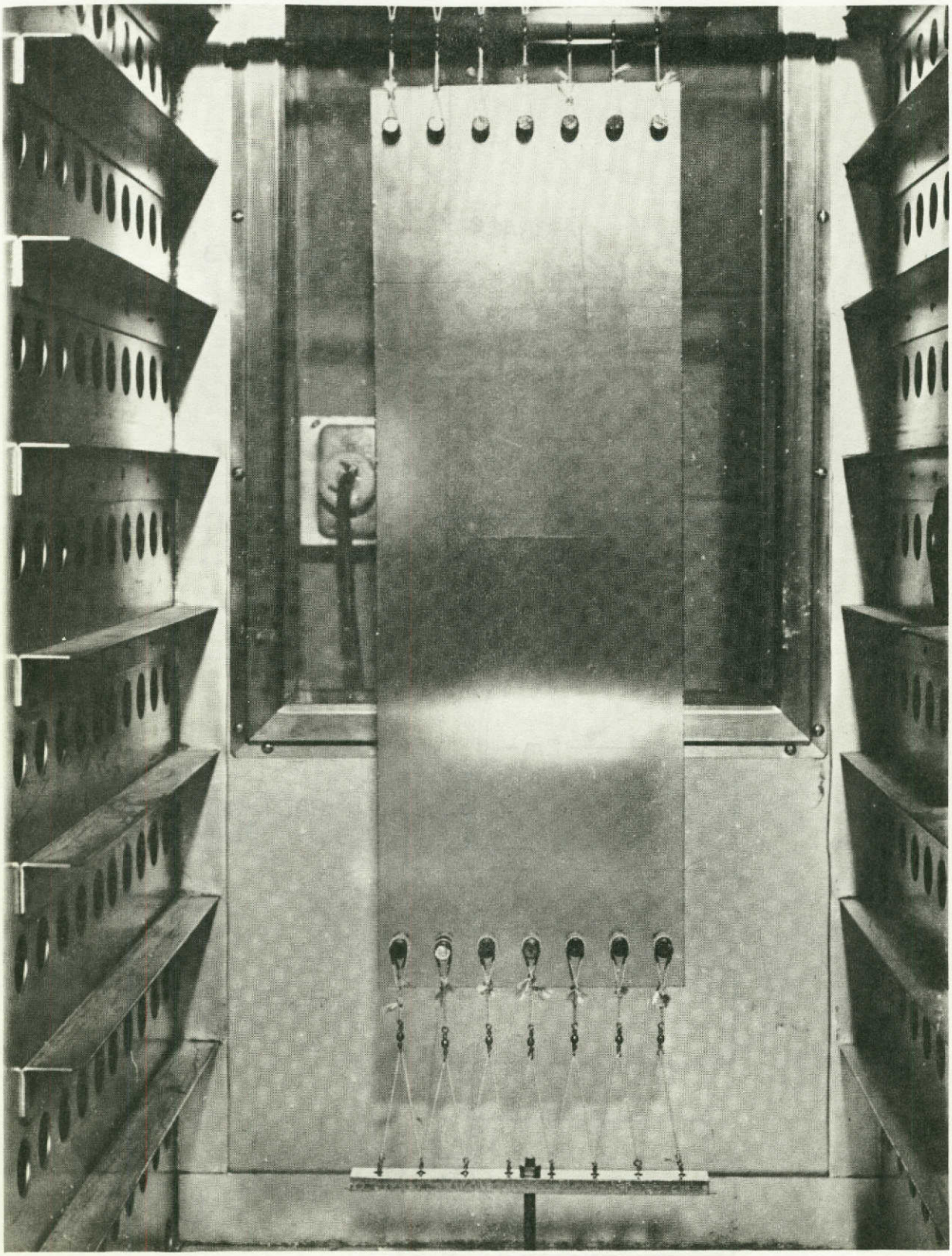

Figure 3. Photo of Test Set-up.

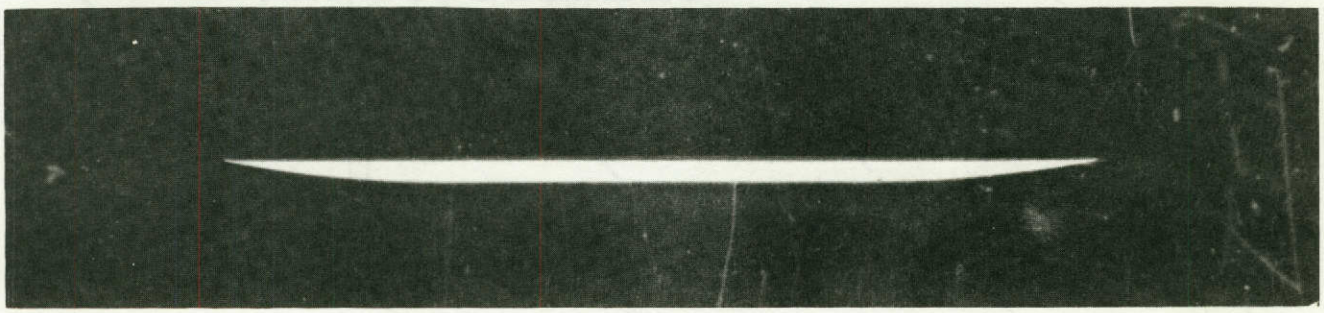

Figure 4. Flaw After Stress Freezing

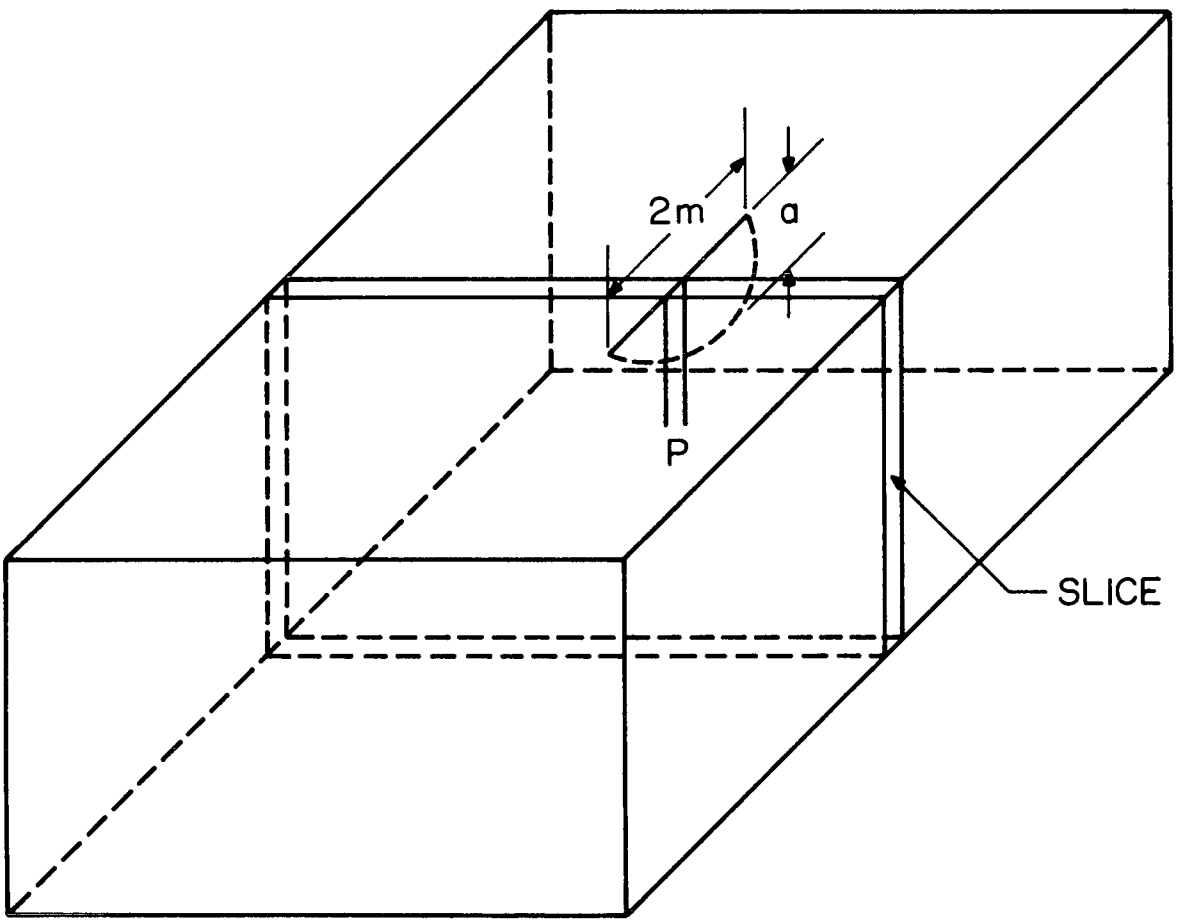

Figure 5. Slice Orientation

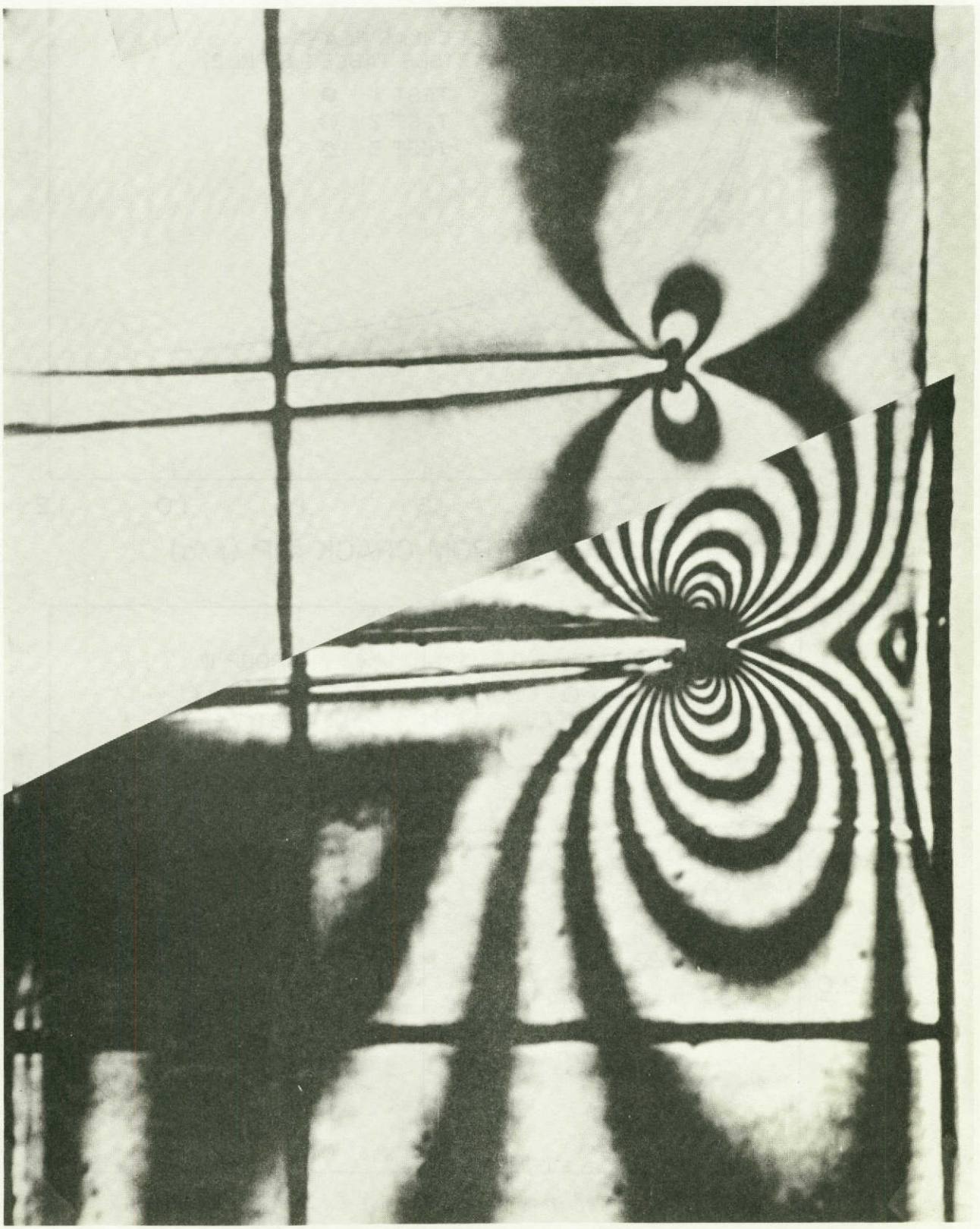

Figure 6. Fringe Photos Multiplied and Unmultiplied (Fifth Multiple) 16X

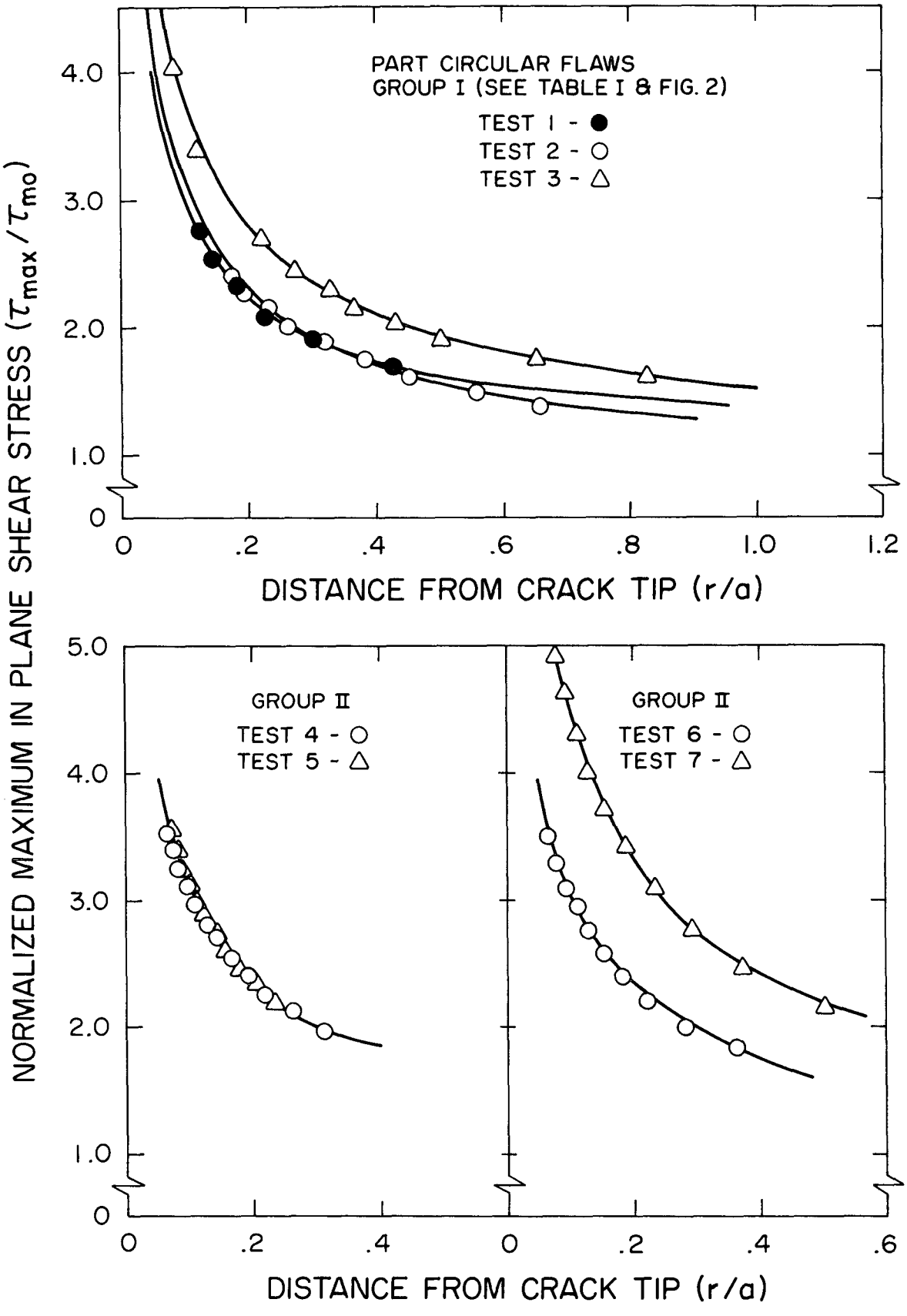

Figure 7. Raw Data τ_m/τ_{mo} vs. r/a

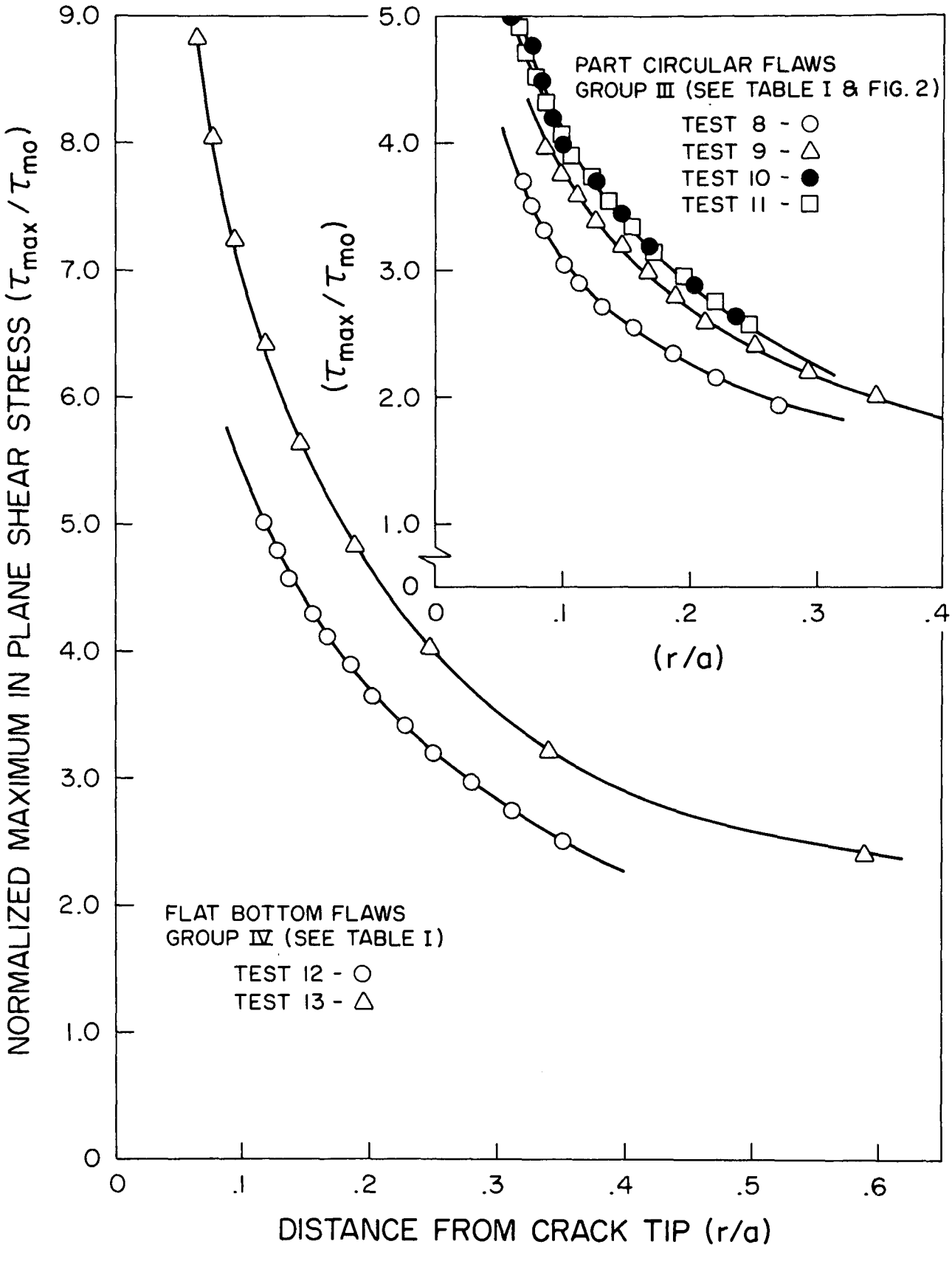

Figure 8. Raw Data τ_m/τ_{mo} vs. r/a

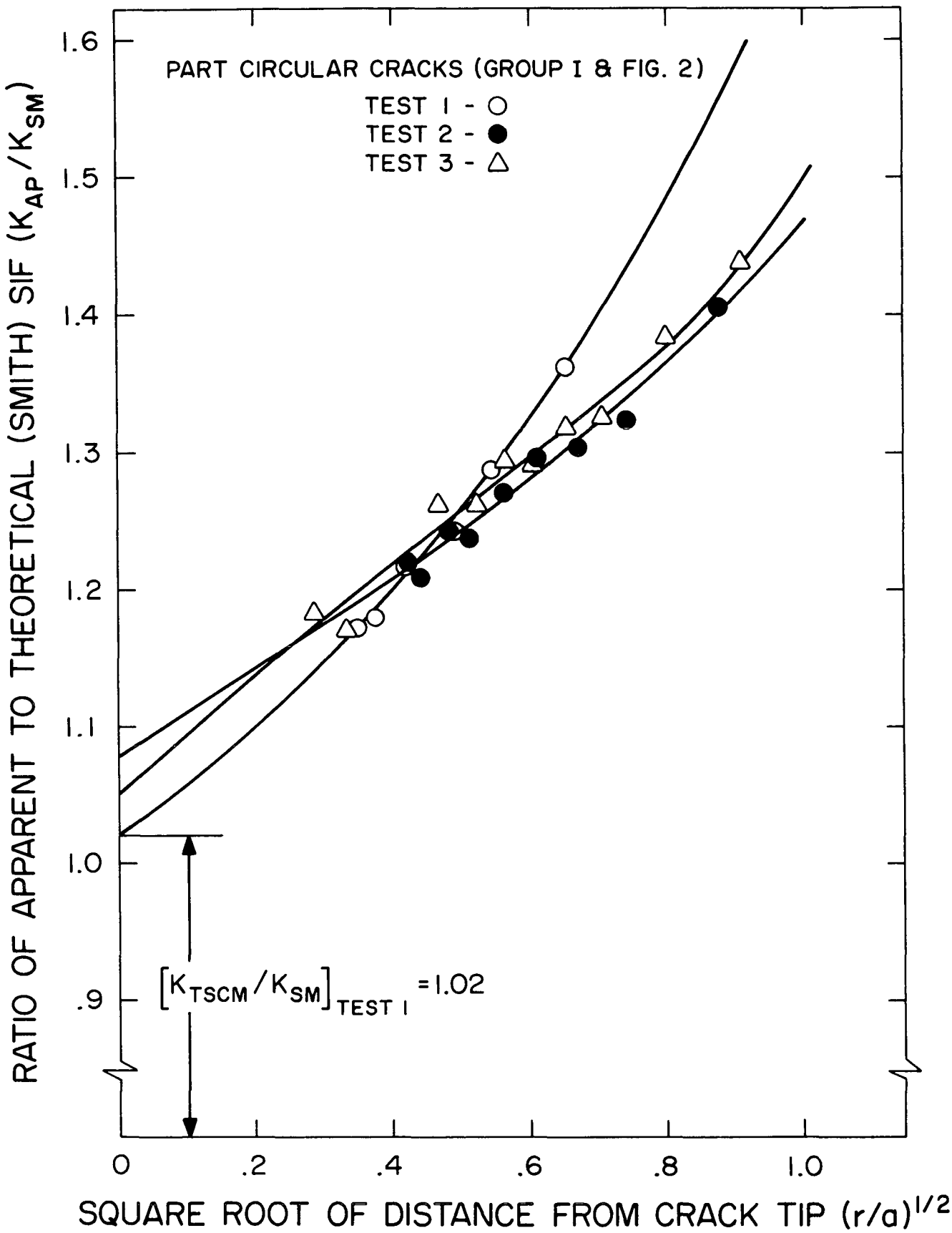

Figure 9. K_{Ap}/K_{Sm} vs. $(r/a)^{1/2}$ TSCM

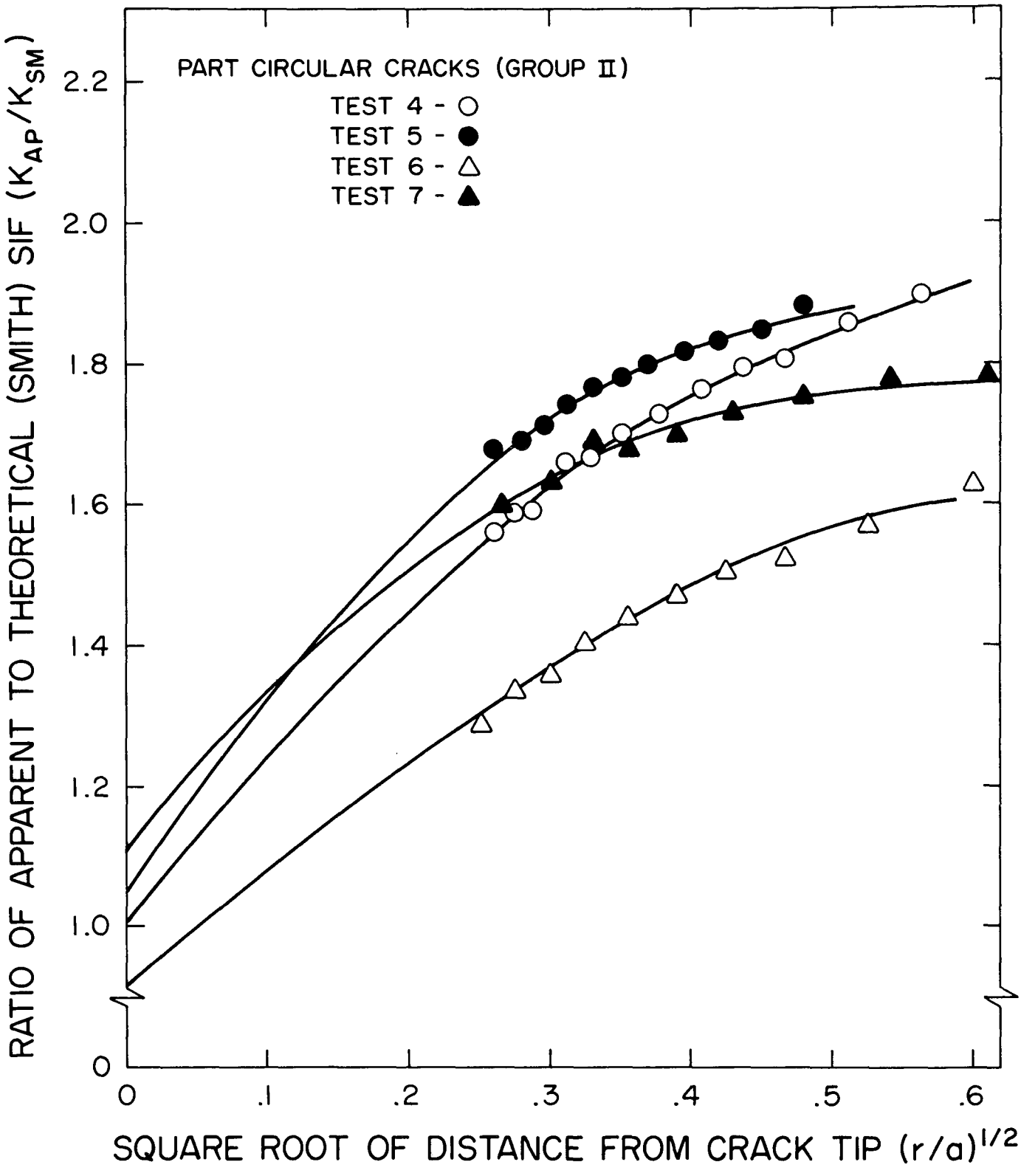

Figure 10. K_{Ap}/K_{Sm} vs. $(r/a)^{1/2}$ TSCM

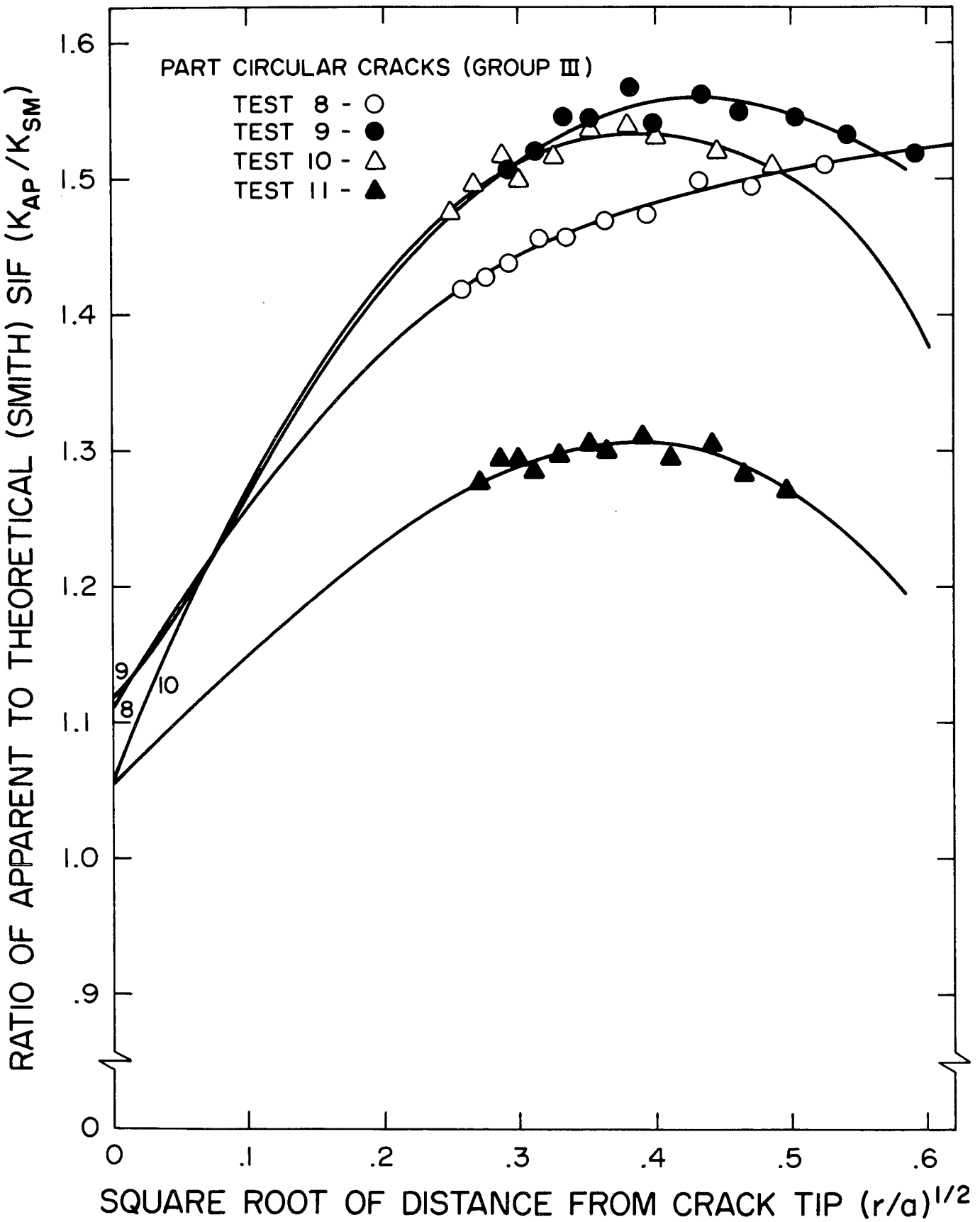

Figure 11. K_{Ap}/K_{Sm} vs. $(r/a)^{1/2}$ TSCM

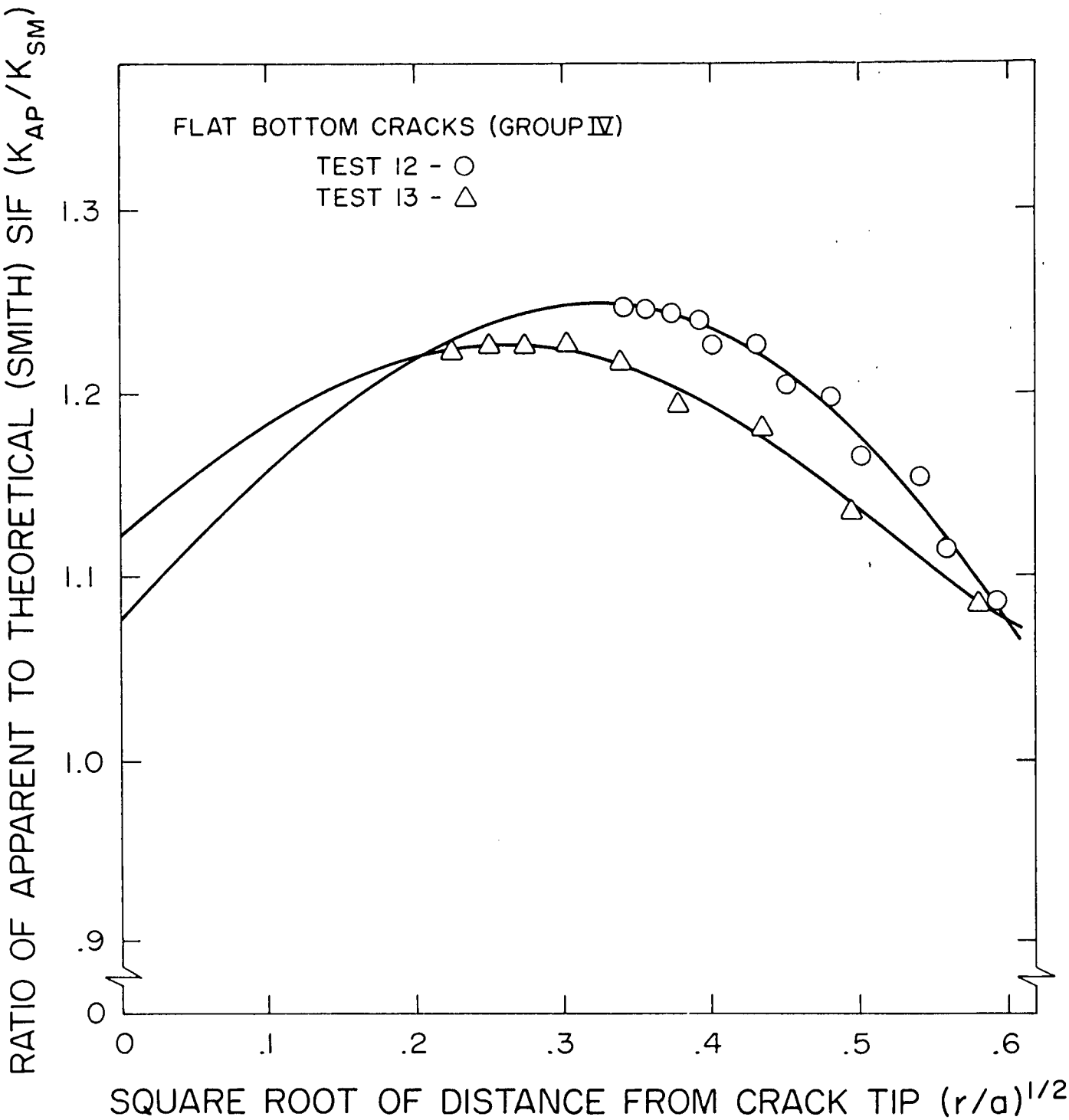

Figure 12. K_{Ap}/K_{Sm} vs. $(r/a)^{1/2}$ TSCM

TABLE I Data and Results

Group	I			II				III				IV	
Test #	1	2	3	4	5	6	7	8	9	10	11	12[a]	13[a]
Part Circular Flaw Length 2m, inches	1.500	0.881	1.199	1.423	1.585	1.989	1.630	1.580	2.018	1.899	1.554	2.004	3.000
Radius of Penetrating Circle, A, inches	1.507	0.882	1.500	0.883	1.000	1.506	1.503	0.995	1.500	1.503	1.500	1.500	1.500
Max Flaw Depth a, inches	0.200	0.118	0.125	0.360	0.390	0.375	0.240	0.390	0.390	0.337	0.217	0.213	0.219
Plate Thickness, t, inches	0.779	0.473	0.502	0.811	0.781	0.795	0.480	0.520	0.552	0.448	0.288	0.284	0.292
Remote Stress, $\bar{\sigma}$, psi	13.2	19.1	12.3	13.3	14.9	13.8	13.8	13.2	11.9	13.6	13.5	11.2	6.94
Material Fringe Value F, lbs/inches/order	1.53	1.40	1.52	1.51	1.53	1.53	2.60	1.52	1.52	2.27	1.52	1.52	1.52
Slice Thickness, T, inches	0.039	0.090	0.091	0.080	0.050	0.043	0.061	0.059	0.064	0.063	0.095	0.099	0.136
a/t	0.257	0.250	0.249	0.444	0.499	0.472	0.500	0.750	0.706	0.752	0.754	0.750	0.750
Finite Width Correction	1.001	1.000	1.001	1.005	1.007	1.006	1.009	1.011	1.015	1.015	1.009	1.027	1.076
M/Φ (Smith)	1.15	1.18	1.42	0.83	0.86	0.97	1.18	0.96	1.09	1.21	1.40	b	b
M/Φ (Experimental)	1.17	1.28	1.52	0.83	0.90	0.90[c]	1.33	1.07	1.21	1.28	1.48	2.08	2.79
K_I (Experimental), lbs/(inches)$^{3/2}$	12.2	14.9	11.7	11.7	14.8	13.5 [c]	16.0	15.7	15.9	17.9	16.5	19.1	16.1
K_I (Smith Theory), lbs/(inches)$^{3/2}$	12.0	13.8	10.9	11.7	14.1	14.6	14.1	14.0	14.4	16.9	15.6	b	b

TABLE I Data and Results (cont.)

Group	I			II				III				IV	
Test #	1	2	3	4	5	6	7	8	9	10	11	12[a]	13[a]
Equivalent ellipse based upon flaw depth and curvature													
a/2c	0.182	0.183	0.144	0.319	0.312	0.250	0.200	0.313	0.255	0.237	0.190		
M/Φ (Shah-Kobayashi)	0.98	0.96	1.01	0.81	0.84	0.91	0.97	0.92	0.97	1.04	1.11		
M/Φ (Rice-Levy)	~~1.13~~ 0.89	0.90	0.97	0.77	0.81	0.91	1.00	0.30	0.71	0.63	0.71		
M/Φ (Newman)	1.02	1.02	1.06	0.86	0.87	0.97	1.05	0.97	1.13	1.18	1.33		
K_I (Shah-Kobayashi), lbs/(inches)$^{3/2}$	10.2	11.2	7.8	11.5	13.8	13.6	11.6	13.4	12.8	14.5	12.4		
K_I (Rice-Levy), lbs/(inches)$^{3/2}$	~~11.8~~ 7.35	10.5	7.5	10.9	13.3	13.6	12.0	4.3	9.3	8.8	7.9		
K_I (Newman), lbs/(inches)$^{3/2}$	10.7	11.9	8.2	12.2	14.4	14.6	12.6	14.2	16.2	16.5	14.6		
Equivalent ellipse based upon flaw depth and area													
a/2c	0.155	0.156	0.121	0.284	0.277	0.216	0.171	0.277	0.221	0.204	0.162	0.110	0.070
M/Φ (Shah-Kobayashi)	1.00	1.00	1.04	0.86	0.87	0.95	1.02	0.97	1.02	1.09	1.15	1.25	1.31
M/Φ (Rice-Levy)	~~1.20~~ 0.95	0.95	1.01	0.81	0.85	0.97	1.10	0.37	0.83	0.75	0.86	1.17	1.84
M/Φ (Newman)	1.05	1.05	1.10	0.92	0.93	1.03	1.15	1.07	1.22	1.27	1.47	1.70	2.30
K_I (Shah-Kobayashi), lbs/(inches)$^{3/2}$	10.4	11.6	8.0	12.2	14.4	14.2	12.2	14.2	13.5	15.2	12.8	11.4	7.6
K_I (Rice-Levy), lbs/(inches)$^{3/2}$	~~12.5~~ 9.9	11.1	7.8	11.4	14.0	14.6	13.2	5.4	10.9	10.4	9.6	10.7	10.6
K_I (Newman) lbs/(inches)$^{3/2}$	11.0	12.2	8.5	13.0	15.3	15.5	13.8	15.6	17.5	17.7	16.4	15.6	13.3

TABLE I Data and Results (cont.)

Group	I			II				III				IV	
Test #	1	2	3	4	5	6	7	8	9	10	11	12[a]	13[a]
	Equivalent ellipse based upon flaw depth and length												
a/2c	0.133	0.134	0.104	0.253	0.246	0.189	0.147	0.246	0.193	0.178	0.140	0.106	0.073
M/Φ (Shah-Kobayashi)	1.02	1.01	1.12	0.90	0.91	0.98	1.04	1.02	1.07	1.13	1.19	1.22	1.32
M/Φ (Rice-Levy)	~~1.25~~ 0.99	1.00	1.06	0.86	0.90	1.08	1.18	0.48	0.95	0.82	1.05	1.28	1.79
M/Φ (Newman)	1.08	1.08	1.12	0.96	0.96	1.07	1.21	1.15	1.28	1.38	1.56	1.73	2.20
K_I (Shah-Kobayashi), lbs/(inches)$^{3/2}$	10.7	11.8	8.6	12.7	15.0	14.7	12.5	14.9	14.1	15.8	13.3	11.2	7.6
K_I (Rice-Levy), lbs/(inches)$^{3/2}$	~~13.1~~ 10.35	11.600	8.2	12.1	14.9	16.2	14.1	7.0	12.5	11.4	11.7	11.7	10.3
K_I (Newman), lbs/(inches)$^{3/2}$	11.3	12.6	8.6	13.6	15.8	16.1	14.5	16.8	18.3	19.3	17.4	15.8	12.7

36

a Flat bottom flaws

b Smith Theory (equivalent area and depth)

	Test 12	Test 13
K_I, lbs/(in)$^{3/2}$	17.7	14.6
M/Φ	1.93	2.54

Smith Theory (equivalent length and depth)

	Test 12	Test 13
K_I, lbs/(in)$^{3/2}$	16.1	14.2
M/Φ	1.76	2.47

For Groups III and IV, data from Rice-Levy Theory were extrapolated and are not regarded as accurate except in an order of magnitude sense.

K_I (edge crack): Test 12 67.2 lbs/(in)$^{3/2}$

Test 13 42.2 lbs/(in)$^{3/2}$

c Mottling in this test specimen caused a reduction in K_{Exp} of about 10%.